Two new "onium" fluorosilicates, the products of interaction of fluorosilicic acid with 12-membered macrocycles: structures and spectroscopic properties

Vladimir O. Gelmboldt,[a] Eduard V. Ganin,[b] Marina S. Fonari,*[c] Yurii A. Simonov,[c] Larisa V. Koroeva,[a] Alim A. Ennan,[a] Stepan S. Basok,[d] Sergiu Shova,[c] Hanspeter Kählig,[e] Vladimir B. Arion[f] and Bernhard K. Keppler[f]

Received 12th March 2007, Accepted 8th May 2007
First published as an Advance Article on the web 9th May 2007
DOI: 10.1039/b703645k

Two novel compounds, $(L^1H)_2[SiF_6]\cdot 2H_2O$ (**1**) and $(L^2H)_2[SiF_5(H_2O)]_2\cdot 3H_2O$ (**2**), resulting from the reactions of H_2SiF_6 with 4′-aminobenzo-12-crown-4 (L^1) and monoaza-12-crown-4 (L^2), respectively, were studied by X-ray diffraction and characterised by IR and ^{19}F NMR spectroscopic methods. Both complexes have ionic structures due to the proton transfer from the fluorosilicic acid to the primary amine group in L^1 and secondary amine group incorporated into the macrocycle L^2. The structure of **1** is composed of $[SiF_6]^{2-}$ centrosymmetric anions, N-protonated cations $(L^1H)^+$, and two water molecules, all components being bound in the layer through a system of NH · · · F, NH · · · O and OH · · · F hydrogen bonds. The $[SiF_6]^{2-}$ anions and water molecules are assembled into inorganic negatively-charged layers *via* OH · · · F hydrogen bonds. The structure of **2** is a rare example of stabilisation of the complex anion $[SiF_5(H_2O)]^-$, the labile product of hydrolytic transformations of the $[SiF_6]^{2-}$ anion in an aqueous solution. The components of **2**, *i.e.*, $[SiF_5(H_2O)]^-$, $(L^2H)^+$, and water molecules, are linked by a system of NH · · · F, NH · · · O, OH · · · F, OH · · · O hydrogen bonds. In a way similar to **1**, the $[SiF_5(H_2O)]^-$ anions and water molecules in **2** are combined into an inorganic negatively-charged layer through OH · · · F and OH · · · O interactions.

Introduction

The products of reaction of fluorosilicic acid (FSA) with organic bases, the fluorosilicates of the relevant "onium" cations, find application as inorganic–organic hybrid functional materials,[1] ionic liquids[2] and reagents for modified zeolite catalytic agents,[3–5] and in the synthesis of silicon tetrafluoride complexes,[6,7] in the production of fungicides,[8] and in the preparation of herbicide-containing mixtures.[9] In addition, these compounds are of interest for the stabilisation of various fluorido complexes of silicon, the products of the hydrolytic transformations of FSA.[10,11] The equilibria in the FSA solution, and number and composition of the co-existing silicon fluorido complexes, still remain a subject of debate.[10–12] The most effective reagents for the selective stabilisation of certain silicon fluorido complexes still remain 18-membered crown- and azacrown-ethers. In particular, the labile products of hydrolytic transformations of the $[SiF_6]^{2-}$ anion, *viz.* complexes $[SiF_5(H_2O)]^-$, $[SiF_5]^-$ and *trans*-$[SiF_4(H_2O)_2]$, have been stabilised in the solid state and structurally described as host–guest complexes with aza- and 1,10-diaza-18-crown-6,[13] *cis*,*syn*,*cis*-dicyclohexyl-18-crown-6[14] and 18-crown-6,[15,16] respectively. It is noteworthy that the smaller 1,7-diaza-15-crown-5[17] and azamacrocycles[18] exclusively form the anhydrous or hydrated ammonium hexafluorosilicates.

It should, however, be noted that the complexing ability of other macrocycles, *e.g.* 12-crown-4 and its substituted derivatives in the reaction with FSA remains practically unexplored. The present study is carried out in continuation of our previous systematic investigations[11,19] and is devoted to the specific features of FSA complex formation with the macrocyclic ligands. We report herein the synthesis, spectroscopic characterisation and structural organisation of compounds resulting from the reaction of FSA with two 12-membered macrocycles, 4′-aminobenzo-12-crown-4 (L^1) and monoaza-12-crown-4 (L^2) (Scheme 1).

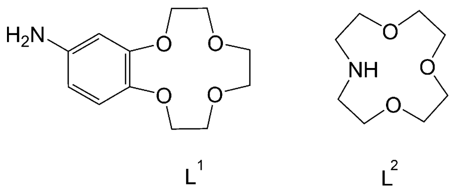

Scheme 1 12-Membered crown ethers used in this study.

Results and discussion

Synthesis

4′-Aminobenzo-12-crown-4 (L^1) was prepared in 3 steps from pyrocatechol following the modified Pedersen procedure.[20]

---

[a] *Physico-Chemical Institute of Environment and Human Protection, Ministry of Education and Science of Ukraine and National Academy of Sciences of Ukraine, Preobrazhenskaya str., 3, 65026, Odessa, Ukraine. E-mail: eksvar@ukr.net*
[b] *Odessa State Environmental University, Lvovskaya str., 15, 65016, Odessa, Ukraine*
[c] *Institute of Applied Physics, Academy of Sciences of Moldova, Academy str. 5, MD2028, Chisinau, Moldova. E-mail: fonari.xray@phys.asm.md*
[d] *A. V. Bogatsky Physico-Chemical Institute, National Academy of Sciences of Ukraine, Lustdorfskaya doroga 86, 65080, Odessa, Ukraine*
[e] *Institute of Organic Chemistry of the University of Vienna, Währingerstr. 38, A-1090, Vienna, Austria*
[f] *Institute of Inorganic Chemistry of the University of Vienna, Währingerstr. 42, A-1090, Vienna, Austria*

Aza-12-crown-4 (L^2) was obtained following the protocol reported in the literature.[21] Compounds **1** and **2** were synthesised by mixing a methanol solution of the corresponding crown ether and an aqueous solution of fluorosilicic acid in a 1 : 3 molar ratio. Crystals suitable for X-ray study were obtained by slow solvent evaporation at room temperature.

Crystal structures

Compound $(L^1H)_2[SiF_6]\cdot 2H_2O$ (**1**) crystallises in the monoclinic space group $P2_1/c$. The asymmetric unit of **1** consists of one half of the hexafluorosilicate anion in partial position on an inversion center, one ammonium-benzo-12-crown-4 cation and one water molecule, both occupying the general positions (Fig. 1). The FSA molecule protonates the primary amine group of the crown ether molecule. Complex **1** is composed of the $[SiF_6]^{2-}$ anion, two macrocyclic cations and two water molecules.

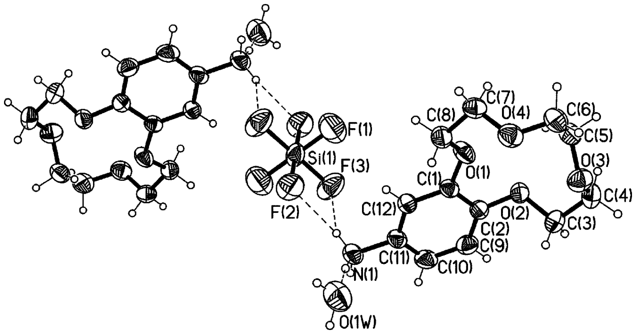

Fig. 1 ORTEP view of **1** with the atom numbering scheme. Displacement ellipsoids are drawn at the 50% probability level. Dashed lines represent the hydrogen bonds.

The components are bound by a network of charge-assisted hydrogen bonds of NH · · · F, NH · · · O and OH · · · F types (Fig. 1). The $[SiF_6]^{2-}$ anion has an usual distorted octahedral geometry with the Si–F distances in the range 1.6588(15)–1.6719(11) Å, F(*cis*)–Si–F(*cis*) bond angles being close to 90° and F(*trans*)–Si–F(*trans*) angles equal to 180°. Each of the $[SiF_6]^{2-}$ octahedra is involved in four bifurcated NH · · · F hydrogen bonds with ammonium groups of four macrocycles and in four OH · · · F hydrogen bonds with four water molecules as multi-center acceptors *via* F(2) and F(3) atoms (Fig. 1, Table 1). The water molecules act as H-acceptors towards the ammonium group *via* a single NH · · · O hydrogen bond, while as H-donors they bridge two symmetry-related $[SiF_6]^{2-}$ anions *via* one single and one bifurcated OH · · · F hydrogen bond. These latter interactions result in the negatively-charged layer (Fig. 2) that runs perpendicular to the [100] direction in the crystal.

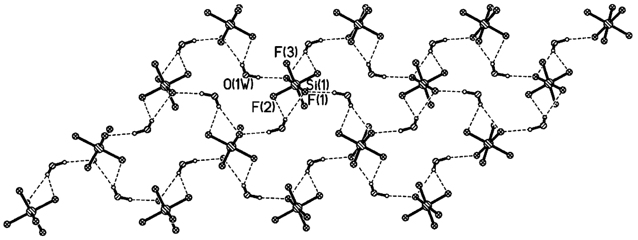

Fig. 2 Fragment of the inorganic negatively-charged layer in **1**.

The macrocyclic ammonium cations are joined *via* NH · · · F and NH · · · O hydrogen bonds in a centrosymmetric mode to the both sides of this inorganic sheet, forming its two hydrophobic surfaces (Fig. 3).

The host–guest complex $(L^2H)_2[SiF_5(H_2O)]_2\cdot 3H_2O$ (**2**) is a quite rare example of stabilisation of the complex anion $[SiF_5(H_2O)]^-$,

Table 1 Hydrogen bonding geometry for **1** and **2**

D–H · · · A	d(D–H)/Å	d(H · · · A)/Å	d(D · · · A)/Å	d(DHA)/°	Symmetry transformation for acceptor
Complex **1**					
N(1)–H(1A) · · · F(3)	0.95(3)	1.86(3)	2.731(2)	151(3)	$x, -y + \frac{1}{2}, z + \frac{1}{2}$
N(1)–H(1A) · · · F(2)	0.95(3)	2.48(3)	3.235(2)	136(2)	$-x, y - \frac{1}{2}, -z + \frac{3}{2}$
N(1)–H(1B) · · · F(2)	0.86(3)	2.10(3)	2.903(2)	156(2)	x, y, z
N(1)–H(1B) · · · F(3)	0.86(3)	2.20(3)	2.883(2)	137(2)	x, y, z
N(1)–H(1C) · · · O(1W)	0.97(2)	1.74(2)	2.701(3)	174(2)	x, y, z
O(1W)–H(1W1) · · · F(1)	0.90(4)	1.91(4)	2.790(3)	166(3)	$x, y, z + 1$
O(1W)–H(1W1) · · · F(2)	0.90(4)	2.60(4)	3.280(3)	133(3)	$-x, -y + 1, -z + 2$
O(1W)–H(2W1) · · · F(1)	0.80(4)	2.24(4)	2.915(3)	143(3)	$x, -y + \frac{3}{2}, z + \frac{1}{2}$
O(1W)–H(2W1) · · · F(2)	0.80(4)	2.26(4)	2.949(3)	145(3)	$x, -y + \frac{3}{2}, z + \frac{1}{2}$
Complex **2**					
N(1)–H(1N1) · · · F(4)	0.83(3)	2.02(3)	2.829(2)	164(2)	x, y, z
N(1)–H(1N1) · · · F(3)	0.83(3)	2.46(2)	2.982(2)	121(2)	x, y, z
N(1)–H(2N1) · · · O(2)	0.83(3)	2.09(3)	2.811(2)	146(2)	x, y, z
N(1)–H(2N1) · · · O(1)	0.83(3)	2.38(3)	2.785(2)	111(2)	x, y, z
N(2)–H(1N2) · · · O(5)	0.86(3)	2.04(3)	2.786(2)	145(2)	x, y, z
N(2)–H(1N2) · · · O(6)	0.86(3)	2.38(3)	2.799(2)	111(2)	x, y, z
N(2)–H(2N2) · · · F(8)	0.86(3)	1.94(3)	2.786(2)	169(2)	x, y, z
N(2)–H(2N2) · · · F(7)	0.86(3)	2.47(3)	3.079(2)	128(2)	x, y, z
O(1W)–H(1W1) · · · F(10)	0.85(4)	1.78(4)	2.629(2)	175(3)	$x, -y - \frac{1}{2}, z + \frac{1}{2}$
O(1W)–H(2W1) · · · O(3W)	0.88(2)	1.72(2)	2.588(2)	171(3)	x, y, z
O(2W)–H(1W2) · · · O(4W)	0.87(2)	1.71(2)	2.569(2)	169(3)	x, y, z
O(2W)–H(2W2) · · · F(3)	0.86(3)	1.77(3)	2.626(2)	172(3)	$x, -y + \frac{1}{2}, z - \frac{1}{2}$
O(3W)–H(1W3) · · · F(7)	0.83(3)	1.97(3)	2.794(2)	172(3)	$x, -y + \frac{1}{2}, z + \frac{1}{2}$
O(3W)–H(2W3) · · · F(9)	0.79(3)	1.96(4)	2.733(2)	168(3)	$-x + 1, y + \frac{1}{2}, -z + \frac{1}{2}$
O(4W)–H(1W4) · · · F(5)	0.84(4)	1.90(4)	2.744(2)	173(3)	$x, -y - \frac{1}{2}, z - \frac{1}{2}$
O(4W)–H(2W4) · · · F(1)	0.79(3)	1.98(3)	2.754(2)	167(3)	$-x, y - \frac{1}{2}, -z + \frac{1}{2}$

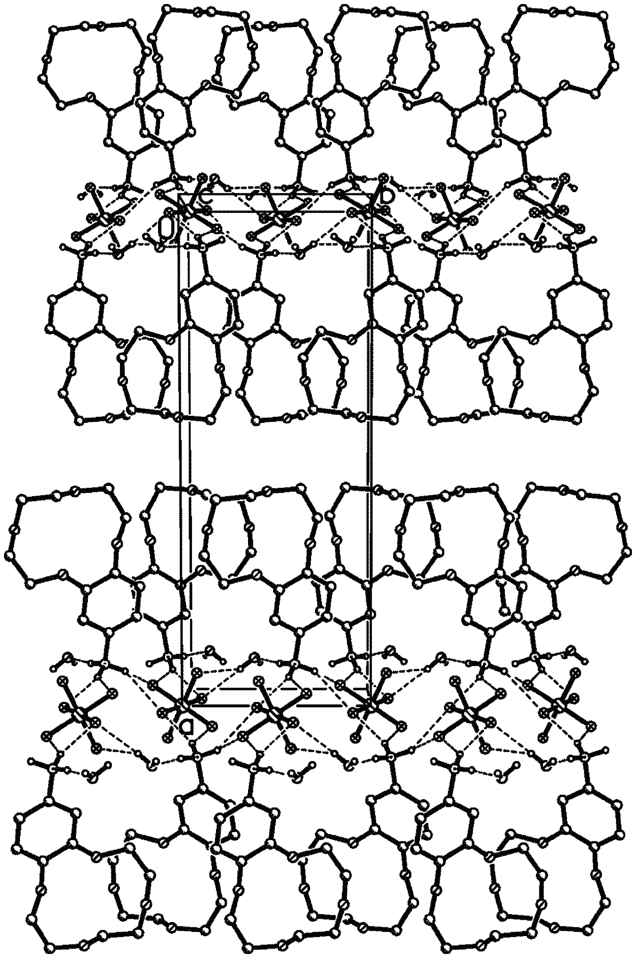

Fig. 3 Packing of the layers in **1**.

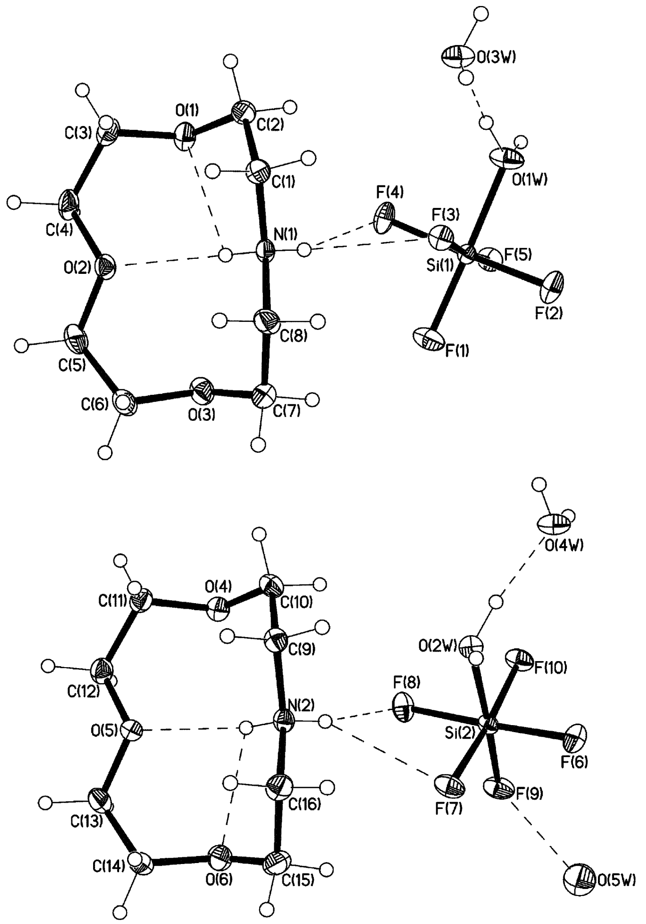

Fig. 4 ORTEP view of two $(\mathrm{L^2H})_2[\mathrm{SiF_5(H_2O)}]_2\cdot3\mathrm{H_2O}$ units in **2** with the atom numbering scheme. Displacement ellipsoids are drawn at the 50% probability level. Dashed lines represent the hydrogen bonds.

the labile product of hydrolytic transformations of $[\mathrm{SiF_6}]^{2-}$. The asymmetric unit of **2** consists of two 12-membered macrocyclic cations, two $[\mathrm{SiF_5(H_2O)}]^-$ anions and three water molecules, one of which, O(5W), has been found to show 25% occupancy. In the crystal each of two crystallographically independent FSA molecules protonates the NH-binding site of the independent macrocycle and is linked with the latter *via* a bifurcated NH···F hydrogen bond (Fig. 4, Table 1) with formation of two neutral units. The second hydrogen of the crown ether ammonium group is directed inside the cavity and is involved in the bifurcated NH···O hydrogen bond responsible for the folded conformation of both cations. The $[\mathrm{SiF_5(H_2O)}]^-$ anion has a distorted octahedral geometry with the Si–F distances in the range 1.6424(12)–1.6979(11) Å. The distances Si–O(H$_2$O) adopt the values 1.8416(15) and 1.8675(14) Å in two independent anions, the F(*cis*)–Si–F(*cis*) bond angles being 87.32(6)–93.94(6)°, F(*trans*)–Si–F(*trans*) angles being in the range 173.21(6)–176.65(7)°, H$_2$O(*cis*)–Si–F(*cis*) angles being 85.99(6)–89.10(6)° and H$_2$O(*trans*)–Si–F(*trans*) angles adopting the values 178.31(7) and 177.89(7)° in two independent anions, respectively (Fig. 4). The geometry of the $[\mathrm{SiF_5(H_2O)}]^-$ anion is in agreement with the reported data.[13,19]

As in **1**, the inorganic anions $[\mathrm{SiF_5(H_2O)}]^-$ and water molecules in **2** form the negatively-charged layers *via* OH···F and OH···O interactions (Fig. 5). The fluoride ligands of both $[\mathrm{SiF_5(H_2O)}]^-$ anions, which are situated in approximately the same plane as those coordinated to the silicon atoms' water molecules, are involved in the intermolecular interactions, and the layer is built up of two alternative ribbons. The first one represents the alteration of five H-bonded unique rings with the following graph set notations:[22] $R_4^4(12)$, $R_3^3(10)$, $R_3^5(12)$ [taking into account non-localised H-atoms of the O(5W) water molecule, the corresponding O(5W)···F(9) and O(5W)···F(9)^i ($i = 1 - x, -1 - y, -z$) separations being 2.664(8) and 2.856(8) Å], $R_4^5(12)$, and $R_3^3(10)$. The next ribbon with the edges shared with the previous one is built up of four unique alternating rings, $R_6^6(16)$, $R_3^3(10)$, $R_4^4(12)$ and $R_3^3(10)$.

As is evident from Fig. 5, the two water molecules coordinated to two silicon atoms [O(1W) and O(2W)] and the two lattice [O(3W) and O(4W)] water molecules use the maximal number of their proton-donor capabilities within the layer: all water molecules act as double donors and all but O(5W) act as single acceptors (*via* coordination or hydrogen bond) within this layer. As we have already noted, this is only the third example of crystal structures that include $[\mathrm{SiF_5(H_2O)}]^-$ anions and protonated N,O-containing macrocycles [those previously reported were complexes $(\mathrm{L^3H\cdot H_2O})[\mathrm{SiF_5(H_2O)}]\cdot\mathrm{H_2O}$ and $(\mathrm{L^4H_2})[\mathrm{SiF_5(H_2O)}]_2$, where $\mathrm{L^3}$ = aza-18-crown-6 and $\mathrm{L^4}$ = 1,10-diaza-18-crown-6].[13] The supramolecular architecture of these related compounds reveals an essential difference: the $\{[\mathrm{SiF_5(H_2O)}]^-\}_2$ units are joined

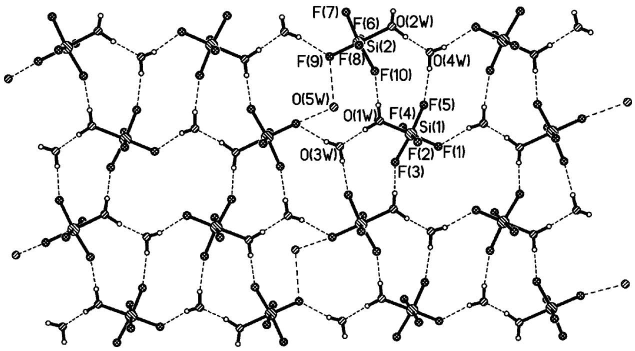

Fig. 5 Fragment of the inorganic negatively-charged layer in **2**.

into centrosymmetric dimers or in chains due to incorporation of lattice water molecules, and the hybrid organic–inorganic layer combines these inorganic motifs and organic cations. Compound **2** is the first example of layer organisation of the negatively-charged species by incorporation of additional lattice water molecules. This leads to different types of anion–anion associations with water molecules mediating the interaction between neighbouring $[SiF_5(H_2O)]^-$ anions.

In a manner similar to **1**, the macrocycles are attached to this inorganic layer using the axial fluoride ligands that are not involved in the intermolecular interactions within the inorganic layer, Fig. 6.

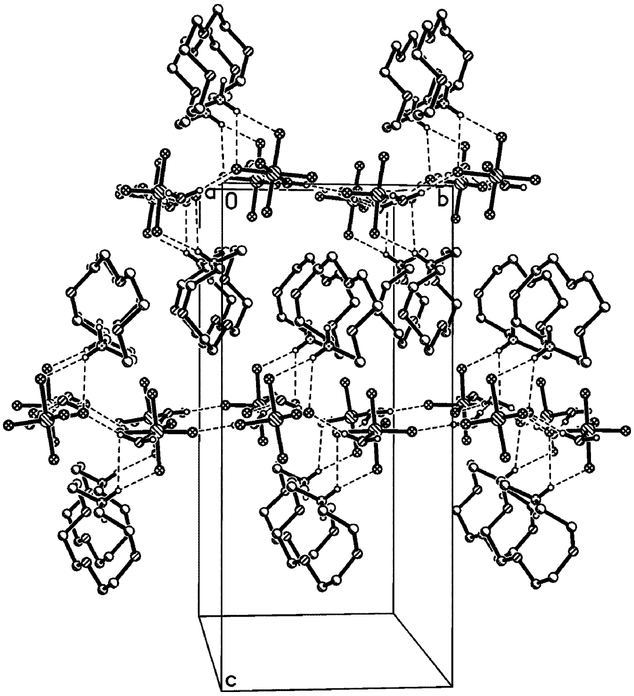

Fig. 6 Packing of the layers in **2**.

It is well known that FSA does not exist as an individual anhydrous compound H_2SiF_6.[23] It crystallises as low-stability hydrates of the general formula $H_2SiF_6{\cdot}nH_2O$ ($n = 4, 6, 9.5$), which represent the oxonium salts of composition $(H_5O_2)_2SiF_6$, $(H_5O_2)_2[SiF_6]{\cdot}2H_2O$ and $(H_5O_2)_2[SiF_6]{\cdot}4.5H_2O$.[24] Recently, the relatively stable (mp ≥60 °C) "simplest hydrate" $H_2SiF_6{\cdot}2H_2O$ was obtained, and its structure was described as an oxonium hexafluorosilicate, $(H_3O)_2[SiF_6]$.[25] Despite its high symmetry (O_h), the hexafluorosilicate anion may be a suitable component for ionic liquids when paired with an appropriate linear or planar base. The family of hexafluorosilicates of aromatic bases is restricted to a few examples[26–29] with different networks of hydrogen bonding in these compounds resulting in different final supramolecular architectures. Thus, in complexes $[o\text{-}CH_3O(O)CC_6H_4NH_3]_2[SiF_6]$[26] and $[o\text{-}C_6H_4(NH_3)_2]_2[SiF_6]$[29] all fluoride ligands of the $[SiF_6]^{2-}$ anions are involved in hydrogen-bonding. In the case of $[o\text{-}CH_3O(O)CC_6H_4NH_3]_2[SiF_6]$ the components form chains, and the chains are involved in stacking interactions *via* benzene rings. The general topology of the structure $[o\text{-}C_6H_4(NH_3)_2]_2SiF_6$ corresponds to a 2D network formed by $[o\text{-}C_6H_4(NH_3)_2]^{2+}$ cations and $[SiF_6]^{2-}$ anions. The hydrates of *p*-bromoanilinium hexafluorosilicate and *p*-toluidinium hexafluorosilicate[28] both also form 2D structures, where the hexagonal H-bonded network built up of $[SiF_6]^{2-}$ anions, ammonium cations and bridging water molecules is surrounded in a centrosymmetric manner by the aromatic rings of the cations arranged perpendicular to the inorganic network and forming two hydrophobic layer surfaces.

The use of 4-aminobenzenesulfonamide or the 4-aminobenzoic acid in the reaction with fluorosilicic acid results in the corresponding ammonium hexafluorosilicates[29] with a complex system of hydrogen bonding that combines the components into a 3D grid. The presence of a tetrahedral ammonium group in L^1 provides the only 2D supramolecular architecture in **1**. In the crystal structure there are no interactions between H-donor groups and oxygen atoms of the polyether ring, indicating that **1** is not a host–guest complex. Instead, it can be categorised as the salt-like adduct of functionalised arylammonium cation. The starting thermolysis temperature, t_0, for compound **1** and for a number of hexafluorosilicates of *ortho*-substituted anilinium hexafluorophosphates[26] (Table 3) has been determined, showing a correlation between the t_0 values and pK_a values of the corresponding arylamines.

It is worth noting that none of the products resulting from reactions of crown ethers or their aza-analogues with FSA are inclusion complexes.[11,19] The interaction between the inorganic "guest" and macrocycle occurs exclusively *via* a net of hydrogen bonds. Therefore the influence of the macrocycle structure on the identity of the extracted from aqueous solution of FSA inorganic species should be considered from the point of view of their ability to form hydrogen bonds. Starting from different macrocycles, we succeeded to stabilise (along with $[SiF_6]^{2-}$) the labile products of its hydrolytic transformations, *viz.*, $[SiF_5(H_2O)]^-$, $[SiF_5]^-$ and $[SiF_4(H_2O)_2]$. In particular, the homoleptic compounds with equivalently sterically-shielded macrocycle sides, *viz.*, 18-crown-6, 15-crown-5 and 12-crown-4, stabilise selectively the *trans*-$[SiF_4(H_2O)_2]$ species, whereas the *cis,syn,cis*-dicyclohexane-18-crown-6, with non-equivalently shielded macrocycle sides, forms an ionic complex with $[SiF_5]^-$ anion. The observed relationship between the crown-ether structure and the composition of the bound fluoro-containing inorganic complex (molecular or ionic) has also been documented for related "host–guest" systems based on neutral $BF_3{\cdot}H_2O$ and anionic $[BF_4]^-$.[11] Stabilisation of the $[SiF_5(H_2O)]^-$ anion has been observed when azacrown-ethers with the N-to-O ratio in favour of oxygen have been used as "host" molecules and organic bases.

Obviously, in each particular case upon interaction of FSA or similar equilibrium system with the corresponding macrocycle, the species is sequestered from aqueous solution, for which the

Table 2 Crystal data and structure refinement parameters for **1** and **2**

Compound	**1**	**2**
Chemical formula	$C_{24}H_{40}F_6N_2O_{10}Si$	$C_{16}H_{46}F_{10}N_2O_{11}Si_2$
Formula weight	658.67	688.73
Temperature/K	100(2)	100(2)
Wavelength/Å	0.71073	0.71073
Crystal system	Monoclinic	Monoclinic
Space group	$P2_1/c$	$P2_1/c$
a/Å	21.8548(6)	14.8889(7)
b/Å	8.0635(2)	9.3635(5)
c/Å	8.5300(2)	20.3291(9)
β/°	98.599(2)	93.900(3)
V/Å^3	1486.31(7)	2827.6(2)
Z, ρ_{calc}/g cm^{-3}	2, 1.472	4, 1.618
μ/mm^{-1}	0.173	0.247
F(000)	692	1448
θ range/°	1.88–30.82	2.35–27.50
Limiting indices	$-31 \le h \le 31$ $-11 \le k \le 11$ $-12 \le l \le 12$	$-19 \le h \le 19$ $-12 \le k \le 12$ $-26 \le l \le 26$
Reflections collected/unique	33020/4660 [R(int) = 0.0296]	88034/6465 [R(int) = 0.0409]
Goodness-of-fit on F^2	1.111	1.063
Final R indices [$I > 2\sigma(I)$]	$R_1 = 0.0493$, $wR_2 = 0.1370$	$R_1 = 0.0410$, $wR_2 = 0.1148$
R indices (all data)	$R_1 = 0.0752$, $wR_2 = 0.1515$	$R_1 = 0.0512$, $wR_2 = 0.1199$
Largest diff. peak and hole, e Å^{-3}	0.380/−0.335	0.594/−0.380

Table 3 Relationship between the pK_a of arylamines and thermolysis temperatures t_0 of the corresponding arylammonium hexafluorosilicates[26]

Amine	pK_a	t_0/°C
L^1	4.63[a]	190[b]
o-$CH_3OC_6H_4NH_2$	4.49	175
o-$CH_3C_6H_4NH_2$	4.39	135
o-$ClC_6H_4NH_2$	2.64	125
o-$BrC_6H_4NH_2$	2.60	125
o-$CH_3O(O)CC_6H_4NH_2$	2.23	115
o-$HO(O)CC_6H_4NH_2$	2.11	140
o-$O_2NC_6H_4NH_2$	−0.29	100

[a] Calculated value. [b] For the anhydrous form.

most effective stabilisation of the host–guest complex by a net of hydrogen bonding interactions is achieved. In addition, lattice water molecules often act as bridging species between "inorganic" and "organic" fragments with formation of supramolecular architecture of the host–guest complex.

Infrared spectra

Broad bands of medium intensity between 3650 and 3030 cm^{-1} in the IR spectrum of **1** (Table 4) have been assigned to the stretching vibrations of the NH_3^+ groups and water molecules involved in the hydrogen bonding network. The deformation vibrations δ(NH_3) and δ(H_2O) were registered at 1655 and 1620 cm^{-1}, correspondingly. Absorptions at 705, 465 and 440 cm^{-1} were attributed to the ν(SiF) and δ(SiF_2) vibrations of the $[SiF_6]^{2-}$ anion, respectively. The character of absorption changes in the range 1145–1095 cm^{-1}, where the bands assigned to the conformationally-sensitive ν_{as}(COC) vibrations of macrocyclic fragment were registered: instead of the observed for L^1 doublet band of medium intensity at 1145 and 1115 cm^{-1}, an intense band at 1130 cm^{-1} with the shoulder at 1100 cm^{-1} is found for **1**, while the band at 1090 cm^{-1} changes its intensity but not the position. In addition, the vibrations ν_s(COC) appear in the spectrum as an intense singlet at *ca.* 1040 cm^{-1}, instead of two bands of medium and weak intensities at 1060 and 1045 cm^{-1} in the spectrum of L^1. We note that the assignment of the skeleton vibrations of the macrocycle in the spectra of L^1 and **1** (Table 4) was made taking into account the data for the related monobenzo-12-crown-4.[30]

The IR spectrum of **2** (Table 4) shows the ν(NH) vibrations of the protonated secondary amine group and the ν(OH) vibrations of coordinated and lattice water molecules as broad bands of medium intensity with weakly pronounced maxima between 3590 and 3110 cm^{-1}. The position of higher frequency components at 3590 and 3550 cm^{-1} is in line with the X-ray data, indicating the presence of outer-sphere water molecules in **2**. The complex band with a maximum at 1585 cm^{-1} and shoulders around 1725, 1655 and 1625 cm^{-1} was assigned to deformation vibrations δ(H_2O), δ(NH_2) and δ(CNH). Intraligand vibrations of macrocycle attributed to the fragments NCH_2CH_2O and OCH_2CH_2O [ν_{as}(CNC), ν_{as}(COC) in the range 1170–1050 cm^{-1}, and ν_s(COC), ν_s(CNC) and ν(CC), ν(CN) in the range 1050–940 cm^{-1}] were also observed. A marked difference between the IR spectra for L^2 and **2** in the range of the $\nu_{as,s}$(CNC) and $\nu_{as,s}$(COC) vibrations, as well as in the range typical of valence-deformation vibrations of the ligand (1000–800 cm^{-1}) indicates the change of conformation and macrocycle symmetry upon complex formation.

In accordance with the X-ray data, the interpretation of the vibrations of the SiF_5O polyhedron was carried out using an approximation of point group symmetry C_{4v}. Thus, the most intense component (760 cm^{-1}) of the complex absorption band in the range 800–700 cm^{-1} includes the ν(SiF_e) (A_1) vibration, and a clearly pronounced shoulder around 720 cm^{-1} – vibrations ν(SiF_a) (A_1). The band of doubly degenerate vibrations ν(SiF) (E)

View Article Online

Table 4 IR spectral data for **1** and **2** and free organic bases

L^1	**1**	L^2	**2**	
	3560 m	3480 m w	3590 m w	ν(NH), ν(OH)
	3455 m		3550 m w	
3430 m	3415 m w		3400 m w	
3345 m w		3300 m w		
3170 m w	3130 m w		3230 m w	
	3110 sh	3090 m w	3110 sh	
3045 sh	3030 sh			δ(NH_2), δ(OH_2), δ(NH_3), δ(CNH)
	1655 m	1655 sh	1725 sh	
	1620 m	1635 m	1655 sh	
1620 m		1620 m		
			1625 sh	
		1585 sh	1585 s	
1595 s	1585 s			$\nu(CC)_{Ph}$
1555 m	1570 sh			
1510 s	1505 s			
1360 sh	1340 sh	1360 sh	1340 sh	ω(CH_2), τ(CH_2), ω(NH_2), δ(CNH), ω(NH_3), $\nu_s(C_{Ph}\text{-}OC)$, $\nu_{as}(C_{Ph}\text{-}OC)$
1320 m	1320 m			
1295 m				
1275 m	1275 m	1280 s	1285 m	
1240 m	1240 m	1240 s	1240 sh	
1220 sh	1220 sh	1220 sh	1220 s	
1180 m				$\delta(CCH)_{Ph}$, ν_{as}(CNC), ν_{as}(COC), ν_s(COC), ν(CC), ρ(NH_2)
1165 m	1160 sh		1170 sh	
1145 m	1130 s	1130 s	1140 s	
1115 m	1100 sh	1100 s		
1090 sh	1090 m			
1060 m		1070 s	1070 m	
1045 w	1040 m	1055 sh	1050 sh	
1030 s	1025 sh	1020 m	1020 m	
965 m	965 m	930 s	940 m	ν_s(COC), ν_s(CNC), δ(CCH), ρ(CH_2) + ν(CO) + ν (CC), ρ(CH_2) + ν(CO) + ν(CC) + ν(NC)
915 m	920 s		920 sh	
900 m	905 sh	900 s	900 sh	
885 sh	890 w			
870 sh	855 m		850 m	
830 m		840 w		
815 sh	800 sh	820 m	820 sh	
765 m	770 sh	780 m	760 s	$\nu(SiF_{eq})$, $\nu(SiF_a)$, ν(SiF), ρ(NH_2), ρ(NH_3), $\nu_{puls.}$, γ(H_2O)
750 sh	760 sh	755 m	720 sh	
725 sh	705 s	720 sh	680 sh	
620 w	610 sh	620 sh	610 sh	δ(CCO), δ(COC), δ(NCC)
565 w	565 w		565 sh	
530 w	530 w	510 m	510 m	
	465 m		465 m	δ(SiF_2)
	440 sh		420 m	

Abbreviations: w: weak, m: medium, s: strong, sh: shoulder.

is revealed as a shoulder around 680 cm^{-1}. The plane vibrations δ(SiF_4) (*E*) were assigned to the band around 465 cm^{-1}; out-of-plane vibrations δ(SiF_2) (A_1) were registered as a shoulder around 420 cm^{-1}.

^{19}F NMR study on 2

^{19}F NMR spectra for **2** in acetonitrile solution show several signals, some of them being temperature-dependent, typical for systems with fluorine exchange (Fig. 7). Their line widths decrease with decreasing temperature due to the decreased exchange rate. Thus, the spectrum measured at the lowest temperature of 243 K was used for the assignment of the different fluoride complexes (Fig. 8 and Table 5).

The intense singlet at δ −127.86 ppm and a heteronuclear coupling constant $J(^{29}Si,^{19}F) = 108$ Hz corresponds to the $[SiF_6]^{2-}$ anion.[31] Only at 243 K can the silicon satellites be observed, as at higher temperatures the line width exceeds the *J* coupling. Two signals of equal intensity with chemical shift values of −123.81 and −136.05 ppm can be attributed to *cis*-$SiF_4{\cdot}2H_2O$ (Fig. 8). They appear as poorly resolved triplets due to a rather small fluorine coupling constant $J(^{19}F,^{19}F) = 1.3$ Hz at 243 K, which increases

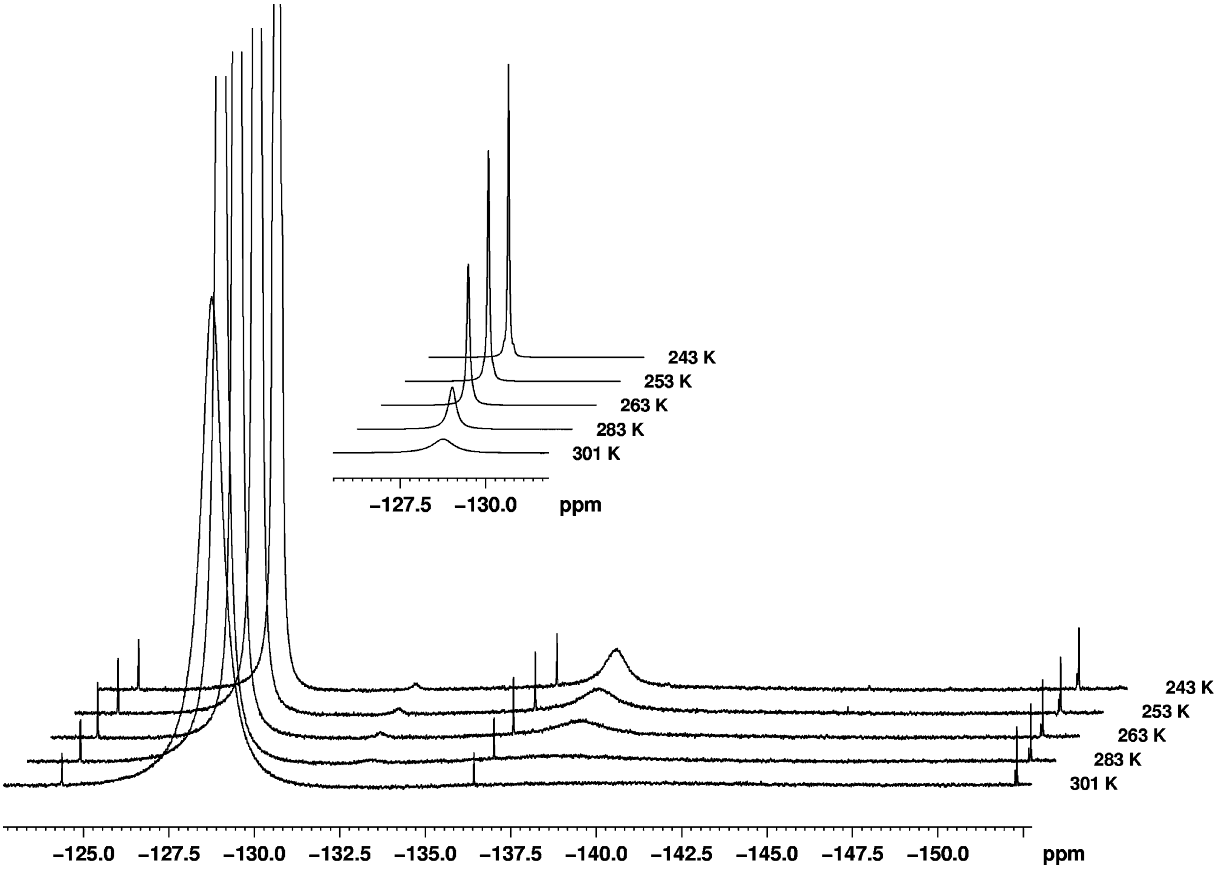

Fig. 7 ^{19}F NMR spectra for **2** at different temperatures (vertical scaling optimised for the minor signals, with the main signal in the inset).

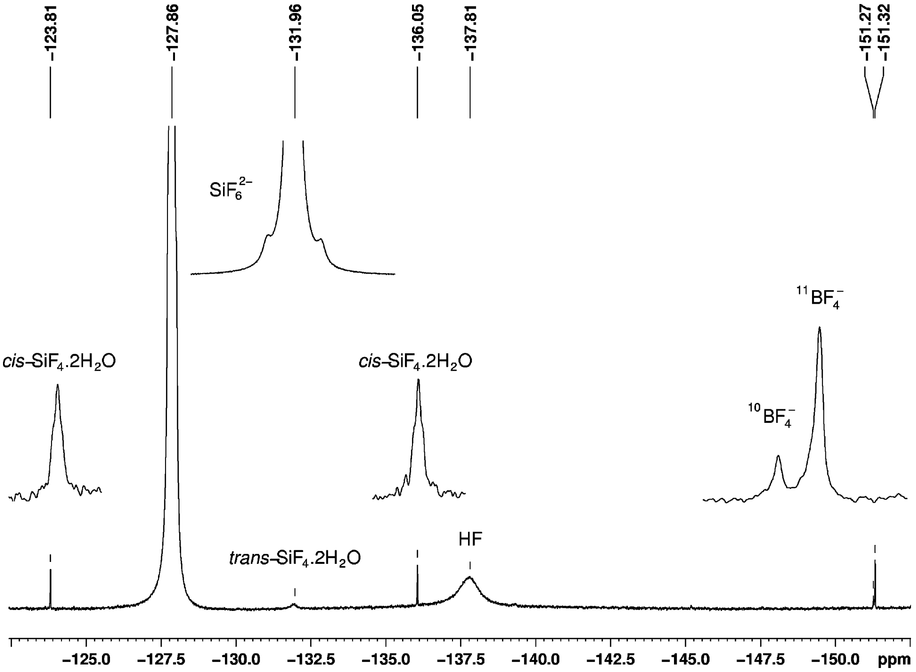

Fig. 8 ^{19}F NMR spectrum of **2** at 243 K.

Table 5 ^{19}F NMR data for complex **2** in CD_3CN at 243 K

Complex	δ(F)/ppm [a]	J/Hz
$[SiF_6]^{2-}$	−127.86	(^{29}Si,^{19}F) 108
trans-$SiF_4 \cdot 2H_2O$	−133.0 (F_c)	
cis-$SiF_4 \cdot 2H_2O$	−123.81[b] (F_c); −136.05[b](F_t)	(^{19}F,^{19}F) 1.3
HF	−137.81	
BF_4^-	−151.27; −152.32	

[a] F_c, F_t: fluorine atoms *cis* and *trans* to H_2O, respectively. [b] Incompletely resolved triplet.

slightly to 2 Hz upon elevating the temperature to 301 K. In addition, as the only fluorine–silicon species, these signals exhibit the same sharp line over the whole measured temperature range.

The signal with the chemical shift δ(F) around 131.96 ppm can presumably be referred to the *trans*-isomer. The assignment has been made taking into account the closeness of the chemical shifts of *cis*- and *trans*-$SiF_4 \cdot 2H_2O$ with those of isomeric complexes $SiF_4 \cdot 2DMSO$ with an analogous O-donor.[32] The *cis*-isomers of SiF_4 with the molecular N-donors show ^{19}F signals for the vector N–Si–F shifted to higher fields.[33,34] The broad signal with the chemical shift at −137.8 ppm is probably due to HF or exchange interaction between HF, F^- and HF_2^-,[31] formed as a result of hydrolytic transformations of fluorido complexes. The strong field signals at −151.27 and −151.32 ppm with relative intensities of 1 : 4 refer to the anion BF_4^- [35] (resonance $^{10}BF_4^-$ and $^{11}BF_4^-$ correspondingly, with a chemical shift difference between the two signals of about 20 Hz as the sequence of the isotopic shift ^{10}B–^{11}B), which is probably formed as a by-product by reaction of HF with the borosilicate glass of the NMR tube.[34]

The results obtained may be interpreted as follows: the labile anions $[SiF_5(H_2O)]^-$ formed from the weak Lewis acid (SiF_5^-) and weak Lewis base (H_2O) as a result of the first step of the hydrolysis of SiF_6^{2-} anions in solutions of FSA[10] can be stabilised in the solid state as host–guest complexes with the protonated forms of azacrown ethers. The system of charge-assisted hydrogen bonds serves as a stabilising basis for complex **2** and related compounds reported previously, *e.g.* $(L^3H \cdot H_2O)[SiF_5(H_2O)] \cdot H_2O$ and $(L^4H_2)[SiF_5(H_2O)]_2$ (L^3 = aza-18-crown-6, L^4 = 1,10-diaza-18-crown-6). Upon dissolution in the absence of that stabilising factor the anions $[SiF_5(H_2O)]^-$ disproportionate according to eqn (1):

$$2[SiF_5(H_2O)]^- \rightarrow [SiF_6]^{2-} + [SiF_4(H_2O)_2] \qquad (1)$$

with the formation of a more stable $[SiF_6]^{2-}$ anion and $[SiF_4(H_2O)_2]$ complex. The last species may undergo further hydrolysis with the participation of the outer-sphere water molecules according to eqn (2):

$$[SiF_4(H_2O)_2] + H_2O \rightarrow SiO_2 \cdot H_2O + 4HF \qquad (2)$$

This, together with the volatility of the diaqua-complex, probably explains the rather low content of *cis*- and *trans*-$SiF_4 \cdot 2H_2O$ in acetonitrile solution. We note here that the complex $SiF_4 \cdot 2H_2O$, which is a strong Brønsted acid,[36] is relatively stable only in highly acidic solutions of FSA; the decrease of solution acidity results in the hydrolytic decomposition of the complex.

It should be also noted that ^{19}F NMR spectroscopy data indicate that $[SiF_4(H_2O)_2]$ is present in acetonitrile solution in the form of two geometric isomers. Previously,[15,16] we succeeded to stabilise and describe the crystal structure of the *trans*-$[SiF_4(H_2O)_2]$ isomer isolated in the solid state as a host–guest complex of composition (*trans*-$SiF_4 \cdot 2H_2O$)·18-crown-6·$2H_2O$. The possibility for $SiF_4 \cdot 2H_2O$ to exist as *cis*- and *trans*-isomers has been predicted[37] on the basis of gaseous-phase non-empirical calculations for the products of hydrolysis of silicon tetrafluoride. The theoretical study revealed higher thermodynamic stability (by 5.0 kcal mol^{-1}) for *cis*-$SiF_4 \cdot 2H_2O$ (symmetry C_{2v}) compared to the *trans*-$SiF_4 \cdot 2H_2O$ (symmetry C_i) for the idealised geometries in the gaseous state. The evident influence of the medium (solvation and other factors) on the relative stability of the isomeric forms of $SiF_4 \cdot 2H_2O$ in liquid phase has also been discussed.[37]

Conclusions

A novel 12-membered crown ether, 4′-aminobenzo-12-crown-4 (L^1), has been synthesised using the modified Pedersen procedure. This macrocycle, containing a primary amine group, together with another as-yet poorly exploited 12-membered crown ether, aza-12-crown-4 (L^2), with a secondary amine group incorporated into the macrocyclic framework, were used as ligands in the reaction with fluorosilicic acid. Two novel complexes, $(L^1H)_2[SiF_6] \cdot 2H_2O$ and $(L^2H)_2[SiF_5 \cdot 2(H_2O)]_2 \cdot 3H_2O$, were obtained and studied by IR and ^{19}F NMR spectroscopy and X-ray diffraction methods. In complex **1**, the ligand does not use its macrocyclic function, and the final product belongs to the family of the aromatic ammonium hexafluorosilicates sustained by the plethora of charge-assisted $NH(NH_3^+) \cdots F^-$ and $OH(H_2O) \cdots F^-$ hydrogen bonds. The majority of the bases that belong to various classes of compounds, *e.g.*, arylamines,[26–29] alkylamines,[38,39] propargylamine,[40] nitrogen-containing heterocycles of the piperidine or quinoline type,[39] derivatives of guanine,[41,42] hydrazides, thiosemicarbazides and tetraazamacrocycles,[11] form complexes exclusively with the highly symmetric hexafluorosilicate anion, $[SiF_6]^{2-}$. At the same time, only two examples of stabilisation of the labile complex $[SiF_5(H_2O)]^-$ (present in solutions of FSA) by azacrown ethers have been documented so far.[13] The complex $(L^2H)_2[SiF_5(H_2O)]_2 \cdot 3H_2O$ is only the third example of $[SiF_5(H_2O)]^-$ anion stabilised by complex formation with a protonated N-containing crown ether. The major role in stabilisation of the less symmetric and labile species $[SiF_5(H_2O)]^-$ is played by the multiple H-bonding interactions between "organic" and "inorganic" components of the host–guest complex.

Experimental

General methods

All chemicals were purchased from commercial suppliers and used as received. Elemental analyses were carried out at the Physico-Chemical Institute of Environment and Human Protection, Odessa, Ukraine. EI mass spectra were recorded on an MX-1321 instrument (direct sample injection into the ion source, ionisation voltage 70 eV). Infrared spectra were recorded on a Specord 75IR spectrophotometer (4000–400 cm^{-1}, samples in Nujol mulls, KRS-5 glasses). Thermogravimetric analysis (TGA) and differential thermal analysis were performed simultaneously with an OD-102 Paulik–Paulik–Erdey apparatus, with a 10 °C min^{-1} heating rate in air. All NMR experiments were recorded on Avance spectrometers

(Bruker Biospin GmbH, Rheinstetten, Germany), *i.e.* ^{1}H NMR spectra on a DPX 400 instrument (UltraShield™ Magnet) at a resonance frequency of 400.13 MHz, and ^{19}F NMR spectra on a DRX 400 WB instrument equipped with an ATM-BBO probe (outer coil double tunable for ^{1}H or ^{19}F) at a resonance frequency of 376.5 MHz. Chemical shifts were referenced internally to the residual, non-deuterated solvent signal for ^{1}H, or externally to $CFCl_3$ ($\delta = 0$ ppm) for ^{19}F.

The synthesis of L^1 was performed by catalytic reduction of 4′-nitrobenzo-12-crown-4, resulting from the nitration of the initial benzo-12-crown-4 by 50% nitric acid.

Benzo-12-crown-4 [2,3-benzo-1,4,7,10-tetraoxacyclododeca-2-ene]. The compound was synthesised using the modified Pedersen procedure.[19] To a solution of pyrocatechol (22.0 g, 0.20 mol) in *n*-butanol (300 ml) stirred under inert atmosphere a solution of $LiBr\cdot 2H_2O$ (61.5 g, 0.50 mol) and $LiOH\cdot H_2O$ (17.8 g, 0.42 mol) in water (45 ml) was added. The reaction mixture was brought to reflux and then within 5–10 min 1,8-dichloro-3,6-dioxaoctane (38.5 ml, 0.20 mol) was added. The mixture was allowed to react at this temperature for 28 h. After cooling to room temperature the reaction mixture was acidified by concentrated HCl to pH 3–4, filtered and the filtrate evaporated to dryness. The residue was dissolved in chloroform and washed successively with water, saturated Na_2CO_3 and NaCl solutions. After chloroform removal the resulting product was extracted by boiling heptane (2 × 100 ml). After cooling the combined fractions yielded an oil. The supernatant was decanted. The addition of diethyl ether to the remaining oil produced crystals of dibenzo-24-crown-8, which were filtered off, washed with diethyl ether and dried in air. Yield: 1.2 g (27%), mp 112–113 °C (lit.[20] mp 113–114 °C). The filtrate after evaporation of diethyl ether yielded benzo-12-crown-4, which was purified by distillation *in vacuo*, bp 140–145 °C, mp 43–44 °C. An analytical-grade sample was obtained by re-crystallisation from hexane, mp 44–45 °C, in accordance with the literature data[19] (mp 44–45.5 °C). Yield: 11.7 g (26%).

4′-Nitrobenzo-12-crown-4 [2,3-(4′-nitrobenzo)-1,4,7-tetraoxacyclododeca-2-ene]. To a boiling solution of benzo-12-crown-4 (11.2 g, 0.05 mol) in acetonitrile (15 ml), 56% nitric acid (6.0 ml, 0.075 mol) was carefully added. The reaction mixture was allowed to react at this temperature for 30 min and then poured into the ice–water. The precipitate formed was filtered off, washed with water until neutral pH, dried in air and re-crystallised from ethanol. Yield: 12.4 g (92%), mp 108–109 °C (lit.,[43] mp 105–108 °C).

4′-Aminobenzo-12-crown-4 [2,3-(4′-aminobenzo)-1,4,7,10-tetraoxacyclododeca-2-ene]. In a hydrogenation flask were placed 10% Pd/C (1.0 g) and anhydrous methanol (100 ml). The catalyst was activated by passing a stream of hydrogen through the suspension for 1 h. Then a solution of 4′-nitrobenzo-12-crown-4 in methanol (100 ml) was added and the mixture was hydrogenated for 8–10 h to complete the conversion of the substrate [TLC control, DC-Alufolien Kieselgel 60 F254 "Merck", eluent hexane–acetone (1 : 1) or GC control, DIP, glass column (3 × 1200 mm), 5% SE-30 at Inerton N-Super (0.100–0.125 mm) at 50–250 °C]. The catalyst was filtered off, washed with methanol and the combined methanol fractions were evaporated to dryness. The residue was extracted by boiling *n*-heptane (3 × 200 ml) for 20–25 min. The combined extracts were evaporated to one fourth of the initial volume and cooled to 5–10 °C, producing an oil that crystallised on standing for 12–24 h. The product was thoroughly ground and dried *in vacuo*. Yield: 9.9 g (83%), mp 86–88 °C. ^{1}H NMR ($CDCl_3$) δ 3.6 (s, broad, 2H, NH_2), 3.80 (s, 4H, OCH_2CH_2O), 3.81–3.94 (m, 4H, $ArOCH_2CH_2O$), 4.00–4.16 (m, 4H, $ArOCH_2$), 6.24 (dd, 1H, H6, $J_{2'3'} = 8$ Hz, $J_{3'5'} = 3$ Hz), 6.34 (d, 1H, $H_{5'}$), 6.72 (d, 1H, $H_{2'}$).

Aza-12-crown-4 (L^2). Obtained following the literature protocol.[21]

$(L^1H)_2[SiF_6]\cdot 2H_2O$ (1). To a solution of L^1 (0.24 g, 1.0 mmol) in methanol (10 ml) was added 45% H_2SiF_6 (molar ratio 1 : 3). The resulting solution was allowed to stand at room temperature. Slow evaporation of methanol resulted in almost quantitative formation of a colourless crystalline product, mp ≥180 °C (decomp.). Anal. Calc. for $C_{24}H_{40}F_6N_2O_{10}Si$: C 43.76, H 6.12, F 17.31, N 4.25, Si 4.26%; Found: C 43.71, H 6.16, F 17.38, N 4.33, Si 4.30%. Mass spectrum: $[ML^1]^+$ ($m/z = 239$, $I = 100\%$), SiF_3^+ ($m/z = 85$, $I = 45\%$).

$(L^2H)_2[SiF_5(H_2O)]_2\cdot 3H_2O$ (2). L^2 (0.18 g, 1.0 mmol) in methanol (5 ml) was mixed with 45% H_2SiF_6 in a 1 : 3 molar ratio. The resulting solution was allowed to stand at room temperature. Slow evaporation of methanol resulted in almost quantitative formation of a colourless crystalline product, mp ≥110 °C (decomp.); Anal. Calc. for $C_{16}H_{46}F_{10}N_2O_{11}Si_2$: C 27.90, H 6.73, F 27.59, N 4.07, Si 8.16%; Found: C 27.96, H 6.77, F 27.64, N 4.14, Si 8.23%. Mass spectrum: $[ML^2]^+$ ($m/z = 175$, $I = 4\%$), $[ML^2 - CH_2OH]^+$ ($m/z = 144$, $I = 8\%$), SiF_3^+ ($m/z = 85$, $I = 58\%$).

X-Ray diffraction measurements

Diffraction intensities for two complexes were collected at 100 K on a X8APEX II CCD diffractometer with MoKα radiation ($\lambda = 0.71073$ Å) in φ and ω scan modes. The structures were solved by direct methods and refined by full-matrix least-squares method on F^2 using SHELXS97 and SHELXL97 programs, respectively.[44] Non-hydrogen atoms were refined anisotropically. C-bound hydrogen atoms were placed in geometrically calculated positions, N- and O-(water) bound hydrogen atoms were found from difference Fourier maps and refined isotropically. The hydrogen bonding geometries for complexes **1** and **2** are listed in Table 1, and crystallographic data in Table 2. Crystallographic data (CIF files) for the structural analysis of complexes **1** and **2** have been deposited with the Cambridge Crystallographic Data Centre, CCDC reference numbers 635343 and 635344, respectively. For crystallographic data in CIF or other electronic format see DOI: 10.1039/b703645k).

Acknowledgements

We are thankful to Mr A. Roller for the collection of X-ray diffraction data.

References

1 C. Airoldi and R. F. de Farias, *J. Fluorine Chem.*, 2000, **103**, 53.

2 Y. Katayama, M. Yokomizo, T. Miura and T. Kishi, *Electrochemistry*, 2001, **69**, 834.

3 S. Han, D. S. Shihabi and C. D. Chang, *J. Catal.*, 2000, **196**, 375.

4 D. E. Clark, *US Pat.* 4689137, 1987.

5 E. Benazzi, J.-F. Jolly, J. M. Silva and M. F. Ribeiro, *US Pat.* 6245704 B1, 2001.

6 V. O. Gelmboldt, *Russ. J. Gen. Chem.*, 1987, **57**, 709.

7 V. O. Gelmboldt, *Russ. J. Inorg. Chem. (Transl. of Zh. Neorg. Khim.)*, 1989, **34**, 231.

8 R. C. Sheridan, *US Pat.* 112784, 1989.

9 H. Baltruschat and S. Baltruschat, *World Pat.* WO 02/15694 A2, 2002.

10 E. T. Urbansky, *Chem. Rev.*, 2002, **102**, 2837.

11 V. O. Gelmboldt, L. V. Koroeva, Ed. V. Ganin, M. S. Fonari, Yu. A. Simonov, V. Ch. Kravtsov, J. Lipkowski, V. S. Sergienko and A. A. Ennan, *Russ. J. Coord. Chem.*, 2004, **30**, 198.

12 N. N. Golovnev, V. V. Nogteva and I. I. Golovneva, *Russ. J. Gen. Chem.*, 2003, **73**, 1468.

13 V. O. Gelmboldt, Yu. A. Simonov, Ed. V. Ganin, M. S. Fonari, V. Ch. Kravtsov, A. A. Dvorkin, L. V. Ostapchuk and A. A. Ennan, *Russ. J. Coord. Chem.*, 1996, **22**, 21.

14 V. O. Gelmboldt, Ed. V. Ganin, L. V. Ostapchuk, A. A. Ennan, Yu. A. Simonov, V. Ch. Kravtsov, M. S. Fonari and J. Lipkowski, *Russ. J. Inorg. Chem. (Transl. of Zh. Neorg. Khim.)*, 1999, **44**, 1139.

15 Yu. A. Simonov, Ed. V. Ganin, A. A. Dvorkin, M. S. Fonari, V. O. Gelmboldt and A. A. Ennan, *Supramol. Chem.*, 1994, **3**, 185.

16 V. O. Gelmboldt, Ed. V. Ganin, Yu. A. Simonov, L. V. Ostapchuk, M. S. Fonari, J. Lipkowski, A. A. Dvorkin and A. A. Ennan, *Russ. J. Coord. Chem.*, 1995, **21**, 183.

17 V. O. Gelmboldt, Ed. V. Ganin, L. V. Ostapchuk, A. A. Ennan, Yu. A. Simonov, J. Lipkowski, A. A. Dvorkin and M. S. Fonari, *Russ. J. Inorg. Chem. (Transl. of Zh. Neorg. Khim.)*, 1996, **41**, 1041.

18 (*a*) C. A. Ilioudis, D. A. Tocher and J. W. Steed, *J. Am. Chem. Soc.*, 2004, **126**, 12395; (*b*) Yu. A. Simonov, M. S. Fonari, V. Ch. Kravtsov, V. O. Gelmboldt, Ed. V. Ganin, L. V. Ostapchuk, A. A. Ennan, Yu. A. Popkov and J. Lipkowski, *Russ. J. Inorg. Chem. (Transl. of Zh. Neorg. Khim.)*, 1998, **43**, 1982; (*c*) A. N. Chekhlov, *Russ. J. Inorg. Chem. (Transl. of Zh. Neorg. Khim.)*, 2003, **48**, 931; (*d*) M. S. Fonari, Y. A. Simonov, V. Ch. Kravtsov, V. O. Gelmboldt, Ed. V. Ganin, Yu. A. Popkov and L. V. Ostapchuk, *J. Inclusion Phenom. Mol. Recognit. Chem.*, 1998, **30**, 197; (*e*) S. Mason, J. M. Llinares, M. Morton, T. Clifford and K. Bowman-James, *J. Am. Chem. Soc.*, 2000, **122**, 1814; (*f*) J. A. Aguilar, T. Clifford, A. Danby, J. M. Llinares, S. Mason, E. Garcia-Espana and K. Bowman-James, *Supramol. Chem.*, 2001, **13**, 405; (*g*) M. S. Fonari, V. Ch. Kravtsov, Yu. A. Simonov, Ed. V. Ganin and V. O. Gelmboldt, *Zh. Strukt. Khim.*, 1999, **40**, 1002; (*h*) L. Q. Tang, M. S. Dadachov and X. D. Zou, *Z. Kristallogr. – New Cryst. Struct.*, 2001, **216**, 391; (*i*) Md. A. Hossain, J. M. Llinares, S. Mason, P. Morehouse, D. Powell and K. Bowman-James, *Angew. Chem., Int. Ed.*, 2002, **41**, 2335; (*j*) Md. A. Hossain, P. Morehouse, D. Powell and K. Bowman-James, *Inorg. Chem.*, 2005, **44**, 2143; (*k*) M. Szafran, Z. Dega-Szafran, A. Addlagatta and M. Jaskolski, *J. Mol. Struct.*, 2001, **598**, 267; (*l*) G. Rother, H. Worzala and U. Bentrup, *Z. Kristallogr.*, 1997, **212**, 310.

19 Yu. A. Simonov, J. Lipkowski, M. S. Fonari, V. Ch. Kravtsov, ed. V. Ganin, V. O. Gelmboldt and A. A. Ennan, in: *Molecular Recognition and Inclusion* from the Proceedings of the Ninth International Symposium on Molecular Recognition and Inclusion, Lyon, 7–12 September, 1996, ed. A. W. Coleman, Kluwer Academic Publishers, Dordrecht, The Netherlands, 1998, p. 503.

20 C. J. Pedersen, *J. Am. Chem. Soc.*, 1967, **89**, 7017.

21 M. J. Calverley and J. Dale, *Acta Chem. Scand., Ser. B*, 1982, **36**, 241.

22 (*a*) M. C. Etter, *Acc. Chem. Res.*, 1990, **23**, 120; (*b*) J. Bernstein, R. E. Davis, I. Shimoni and N.-L. Chang, *Angew. Chem., Int. Ed. Engl.*, 1995, **34**, 1555.

23 W. W. Wilson and K. O. Christe, *J. Fluorine Chem.*, 1982, **19**, 253.

24 D. Mootz and E.-J. Oellers, *Z. Anorg. Allg. Chem.*, 1988, **559**, 27.

25 V. O. Gelmboldt, Ed. V. Ganin, L. Ch. Minacheva and V. S. Sergienko, *Russ. J. Inorg. Chem. (Transl. of Zh. Neorg. Khim.)*, 2005, **50**, 143.

26 V. O. Gelmboldt, Ed. V. Ganin, L. V. Koroeva, L. Ch. Minacheva, V. S. Sergienko and A. A. Ennan, *Russ. J. Inorg. Chem. (Transl. of Zh. Neorg. Khim.)*, 2006, **51**, 194.

27 V. O. Gelmboldt, L. V. Koroeva and K. V. Domasevich, *Russ. J. Inorg. Chem. (Transl. of Zh. Neorg. Khim.)*, 2006, **51**, 1653.

28 W. A. Denne, A. McL Mathieson and M. F. Mackay, *J. Cryst. Mol. Struct.*, 1971, **1**, 155.

29 V. O. Gelmboldt, A. A. Ennan, Ed. V. Ganin, Yu. A. Simonov, M. S. Fonari and M. M. Botoshansky, *J. Fluorine Chem.*, 2004, **125**, 1949.

30 A.Yu. Tsivadze, A. A. Varnek and V. E. Khutorsky, *Coordination Compounds of Metals with Crown-Ligands* (in Russian), Nauka, Moscow, 1991.

31 K. O. Christe and W. W. Wilson, *J. Fluorine Chem.*, 1990, **46**, 339.

32 V. O. Gelmboldt and S. P. Petrosyants, *Russ. J. Coord. Chem.*, 1989, **15**, 501.

33 V. O. Gelmboldt, S. P. Petrosyants, L. A. Gavrilova and A. A. Ennan, *Russ. J. Coord. Chem.*, 1987, **13**, 1615.

34 T. Q. Nguyen, F. Qu, X. Huang and A. F. Janzen, *Can. J. Chem.*, 1992, **70**, 2089.

35 V. N. Plakhotnyk, R. Schmutzler, L. Ernst, Yu. V. Kovtun and A. V. Plakhotnyk, *J. Fluorine Chem.*, 2002, **116**, 41.

36 K. Kleboth, *Monatsh. Chem.*, 1969, **100**, 1057.

37 S. K. Ignatov, P. G. Sennikov, B. S. Ault, A. A. Bagatur'yants, I. V. Simdyanov, A. G. Razuvaev, E. Ju. Klimov and O. Gropen, *J. Phys. Chem. A*, 1999, **103A**, 8328.

38 G. J. Reiss, *Acta Crystallogr., Sect. C: Cryst. Struct. Commun.*, 1998, **54**, 1489.

39 B. D. Conley, B. C. Yearwood, S. Parkin and D. A. Atwood, *J. Fluorine Chem.*, 2002, **115**, 155.

40 T. Steiner, *J. Chem. Crystallogr.*, 1997, **27**, 673.

41 X. Zhang, R. Bau, J. A. Sheehy and K. O. Christe, *J. Fluorine Chem.*, 1999, **98**, 121.

42 A. Waśkowska, *Acta Crystallogr., Sect. C: Cryst. Struct. Commun.*, 1997, **53**, 128.

43 S. Shinkai, T. Ogawa, Yu. Kusano, O. Manabe, K. Kikukawa, T. Goto and T. Matsuda, *J. Am. Chem. Soc.*, 1982, **104**, 1960.

44 G. M. Sheldrick, *SHELXS97 and SHELXL97, Programs for solution and refinement of crystal structures*, University of Göttingen, Germany, 1997.